International Journal of Heat and Technology
Vol. 44, No. 3, June, 2026, pp. 1149-1159
Journal homepage: http://iieta.org/journals/ijht

Real-Time Integrated Performance Analysis of Photovoltaic Systems under Environmental Stressors in Baghdad

Sura H. Hassan*, Ghassan A. Bilal, Ali A. Ismaeel

Electromechanical Engineering College, University of Technology- Iraq, Baghdad 10066, Iraq

Corresponding Author Email: eme.19.25@grad.uotechnology.edu.iq

https://doi.org/10.18280/ijht.440322

Received: 2 April 2026
Revised: 15 June 2026
Accepted: 23 June 2026
Available online: 30 June 2026

Keywords:
environment, photovoltaic system, dust, Baghdad, solar energy

ABSTRACT

This study analyzes the performance of photovoltaic (PV) systems in hot, dry environments, focusing on the city of Baghdad. An integrated monitoring system was developed using Arduino Mega and ESP32 controllers to collect environmental and operational data in real time. This system allows for the analysis of the effects of basic variables, including solar radiation intensity, panel temperature, wind speed, relative humidity, and dust accumulation, on electrical production capacity. The results showed that the maximum electrical power reached about 36 W during the late morning hours, then gradually decreased despite the continued increase in solar radiation intensity, due to the negative effect of the panel's high temperature on electrical efficiency. The results also showed that dust accumulation reached approximately 34 milligrams per square meter, resulting in a noticeable decrease in the system's efficiency. Furthermore, a significant deviation between the anticipated and measured irradiances: the simulated values were elevated to 660 W/m^2, while the measured values did not reach 550 W/m^2. This clearly demonstrates an overestimation in the simulated irradiance and highlights the limitations of predictive modeling for this context. Local conditions compared to those used in larger prediction models. The suggested system has also proved to be very effective at assimilating both present and forward model output observations to perform performance evaluation, assess accuracy, and provide enhanced operational support for solar energy systems in harsh weather.

1. INTRODUCTION

Climate change, energy security, and the depletion of fossil fuel reserves are pressing issues and have spurred efforts to develop renewable energy technologies. Nearly 80% of global energy consumption depends on fossil fuels, which are a significant cause of climate change [1, 2]. This has reinforced the growing awareness of the need to transition toward renewable energy, with low environmental impact and almost within reach of achieving unlimited availability. Solar energy is one of the most promising renewable resources [3]. Photovoltaic (PV) technologies are a low-emission alternative to conventional fossil-fuel-based power generation, resulting in negligible environmental impact [4, 5]. Despite having eco-friendly structures at their core, PV systems are responsive to environmental parameters such as solar irradiance, shading, temperature variations, wind speed, humidity/atmospheric moisture, and dust deposition, as well as to the connection between global energy needs and these environmental predictors. Dust is a major contributor to reduced PV system performance, as it forms a layer on module surfaces. Dust deposition impedes heat dissipation, raises module temperatures, and reduces conversion efficiency, thereby increasing hot spots that can damage PV modules [6, 7]. Some empirical studies, such as [8], have tried to quantify the impact of these external factors on the performance of PV [9]. Experimental performance differences were examined across various climate zones, and only dust washing was found to cause about 60% losses with minimal benefit for arid locations. The experiment illustrated that dust loading of 20.7–41.3 g/m² in desert areas decreases PV output by 18% to 40% [10]. They also observed that strong winds lead to lower dust deposition, whereas high humidity increases dust attachment. Hashim and Hassan [11] recorded a temperature coefficient of −0.45%/°C in a grid-connected system in Sudan, indicating the unfavorable effect of desert heat. From simulation and measured results. Illustrates that shading could reduce annual performance from 10 to 30% [12]. Ghazia and Ip also found a reduction in power output of up to 60% in the co-dust at high temperatures [13].

Although many studies have addressed the effects of dirt on PV system performance, much of the available data remains location-specific, and a lack of awareness of dust effects may lead to inappropriate maintenance practices and losses in system efficiency [14, 15]. The operating temperature of the PV unit significantly affects its energy output, as higher temperatures reduce electrical efficiency: only about 20% of solar energy is converted into electricity. In comparison, roughly 80% is lost as heat [16]. Wind speed and direction are other parameters that affect PV system performance by improving convective cooling. Droplet formation and water-layer deposition on surfaces are governed by relative humidity, leading to diminished optical transmittance and long-term deterioration due to moisture leakage [17, 18]. The goal of this study is to examine the effects of temperature, wind, and relative humidity on the performance of aging Monocrystalline PV modules in Iraq. This study used actual operating conditions, by means of field measurements, that may be of much help in investigating the impact on these modules by environmental stressors. Results elucidate the criteria for which inputs to select and the requirement for large data integration for environmental assessments of PV modules. It is in this context that the design and management of a solar system integrated monitoring system designed to integrate all operational and environmental aspects of the solar system is described here. It weaves together real-time measurements and predictive data to condense different states of atmospheric behavior at the solar panel surface into a single, interconnected operating system. This approach increases the precision and completeness of system performance, informs operational/maintenance decisions, and increases the effectiveness of solar energy systems in the face of unfavorable conditions.

The main contribution of this study is the development of an integrated, low-cost PV monitoring system that combines real-time field measurements with forecasted weather data. Unlike conventional systems that primarily monitor voltage, current, power, and basic weather parameters, the proposed system also includes dust concentration, dust accumulation on panels, surface humidity, and image-based surface inspection. This integration enables a direct comparison between measured and forecast conditions, which helps detect local impacts such as dust deposition and microclimatic changes and contributes to improving the reliability of PV performance evaluation under extreme conditions in Baghdad.

2. METHODOLOGIES

2.1 Site description

A legacy PV module using the same technology (Monocrystalline) was used for this research. The test was conducted in Baghdad, in a home garage. The coordinates of this site are approximately 33°18′55.44″N latitude, 44°21′12.12″E longitude, and an altitude of 34 meters. This location is hot in summer and cold in winter, with low humidity most of the year. The PV module is made of Monocrystalline silicon and measures 710 × 510 × 45 mm. Table 1 illustrates the module's parameters for 1000 W/m² irradiation and 25 °C [18].

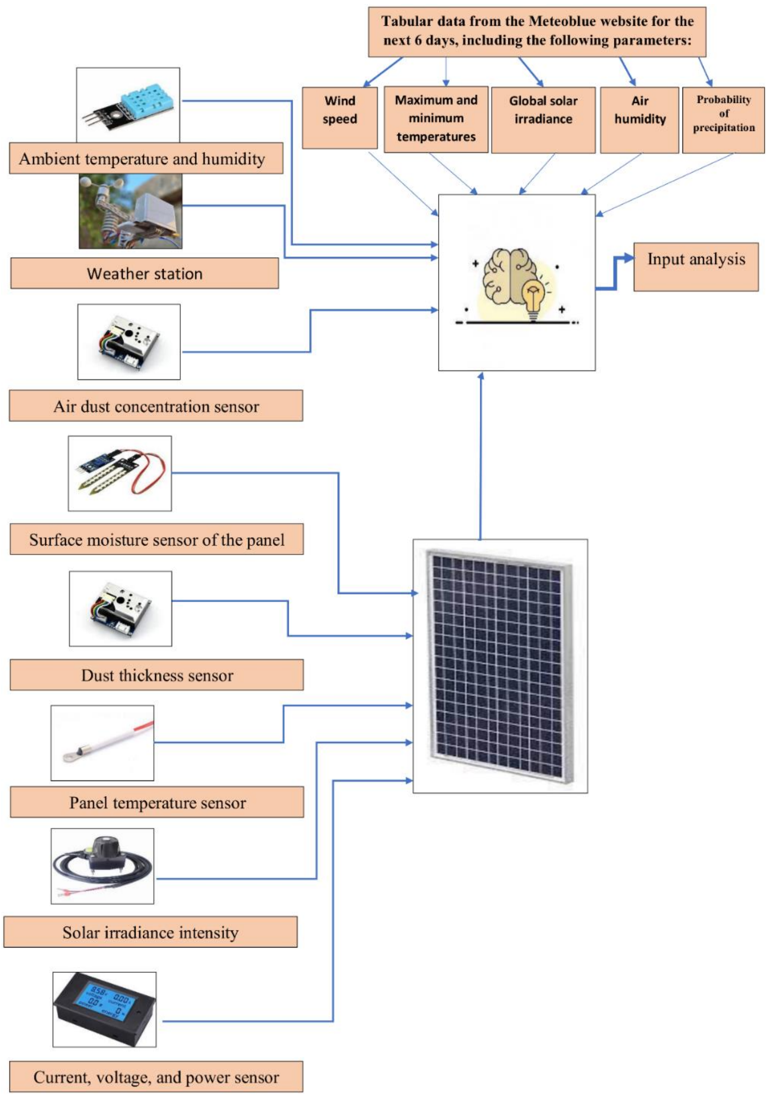

Figure 1. Flow chart for experimental work

Table 1. Characteristics of solar panels

Symbol	Value
Pmax	50 W
Voc	21.0 V
Isc	2.92 A
Vmpp	18 V
Impp	2.7 A
Vsys, max	1000 V
η	21.01%
STC	1000 W/m², 25 ℃, AM 1.5
Tol.	± 3%

2.2 Experimental work

The pragmatic arrangement, as illustrated in Figure 1, is a necessary step toward designing and constructing an integrated system to monitor and diagnose solar panel performance [19]. This is accomplished by combining a multitude of environmental and physical sensors with external data sources, such as those on the Open Meteo website, to obtain information for predictions, thereby enhancing the accuracy of climate change analysis and prediction [20]. The quantized source of production has also been considered in our work through the early detection of factors that affect solar cell efficiency, such as temperature, humidity, dust, radiation, and weather conditions surrounding the solar panel. It can also collect data and write it to an Excel file documenting the solar system's performance, using both real-time and forecast data.

2.2.1 Integrated system

Figures 2 and 3 illustrate the final integrated practical system implemented in this project for monitoring and diagnosing the performance of the solar panel in a realistic operating environment. The realistic images illustrate the test platform after assembly in the field, mounted on a fixed metal base that tilts the solar panel at a 30-degree angle, with the option to adjust the angle, enabling direct receipt of solar radiation while maintaining panel stability during weather changes [6, 21]. It is a way to monitor the intensity of radiation falling on the panel in real time, so as not to lose electric production, which is connected to the actual level of radiation. At the top of the system, it looks like a meteorological station installed on the side of a pole, comprising several sensors to sense the environmental climatic variables, including wind speed, temperature, and humidity, that accurately describe environmental conditions to assist with the data set to translate daily changes into chart production and realistically study the effects of climate on its efficiency. This is essential: the camera at the very top of the aiming column is gray; it points toward the solar panel and periodically takes pictures of its surface to see whether it's working visually. It helps to detect any changes affecting a panel's performance — any dirt or dust accumulating around the solar panels, for instance, or shading some of their cells — since these effects aren't reflected directly in the actual energy readings. Diagnostic reliability is achieved only when the monitoring devices are integrated with the imaging (in systems that support the device on its base) inside a protective box that includes the power and control components, like a solar charge regulator that controls the battery loading and protects it from overcharging or deep discharge; wiring connections connecting the panel to the load and control unit; stable electrical supply systems operating within sensor reality; and the control unit operation. Instability of the supplied electric current is of great importance during the trial period to provide a uniform response b.

Figure 2. Real setup of the experimental system, including photovoltaic (PV) panel, weather station, and camera

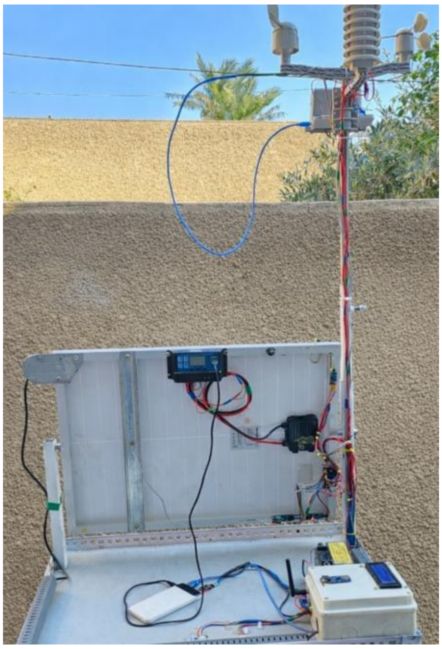

Figure 3. Rear view of the system; the image also illustrates the control box, charge controller, and wiring connections

2.2.2 Control system

As a combination of Arduino Mega 2560 central controller and ESP32 wireless communication module, it is able to process the information instantly from its data. Therefore, the solar panel presence, its performance metrics, and climate factor impact analysis are observed and documented in real-time at a glance. The Open Meteo interface provides a GET request and an analysis of the JavaScript Object Notation (JSON) response through the Arduino JSON library before sending data to Arduino Mega via the Universal Asynchronous Receiver/Transmitter (UART) serial communication protocol on port Serial1 using a logic level converter to convert the signals from 3.3 V to 5 V to protect the Arduino inputs, ensuring the stability of the connections. Moreover, the prediction data comes from the Arduino Mega, which is also the data receiver and organizer for the user. As shown in Figure 4, it is stored on the Secure Digital (SD) card in a Comma-Separated Values (CSV) file in the form of some primitive value as instance of time, temperature, cloud coverage percentage, solar radiation, and wind speed. It functions as a safe storage system that opens and closes files at each line so that missing data will not occur when the power is not running. Conversely, in the system diagram, it can be seen that the control unit is linked to the field sensors, which measure temperature, humidity, wind speed, dust concentration, plate-surface humidity, and radiation intensity, and on the sensors for voltage, current, and power. Meanwhile, important readings show the most important information on the Liquid Crystal Display (LCD) and are stored for later analysis, which ultimately leads to integrating real data with predictive data and carrying out data analysis to support decision making and decide the optimum time for the maintenance work, which also enhances the operational system of the solar system in the field.

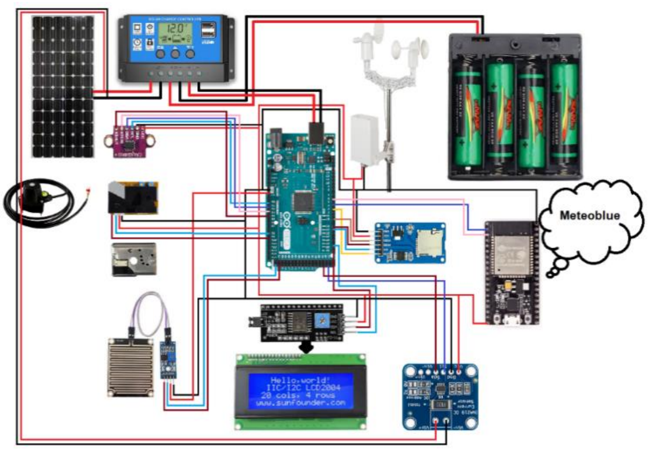

Figure 4. Control system

3. RESULTS FOR THE EXPERIMENTAL DEVICE

This section constitutes an analytic review of the responses achieved concerning the practical part of this research by means of detailing a few graphical curves that prove this way in which the system behaved based on certain rigorous field data measured using sensors; for 11/11/2025, power generation by the solar panel was integrated with climate data imported from Open Meteo database to increase accuracy in how these proposed models came into existence.

3.1 Realistic data results

Figure 5 illustrates the temporal variation in solar radiation and electrical output throughout the day. A gradual increase in radiation and power is observed during the morning, as the angle of incidence of sunlight increases. Radiation reaches its maximum around midday, while electrical power peaks in the late morning. It then gradually decreases despite radiation remaining at relatively high levels, a behavior attributed to the effect of high temperatures on solar cells and the accompanying decrease in efficiency. As daylight hours progress toward evening, both radiation and power decrease significantly as the sun's angle declines and direct radiation diminishes, until production reaches nearly zero at sunset.

Figure 6 illustrates Daily changes in solar radiation, panel surface humidity, and atmospheric humidity. It is noted that the radiation intensity rises rapidly during the morning hours to reach its maximum values at midday and then begins to gradually decrease towards the evening, while atmospheric humidity records high values in the early morning and then decreases with increasing temperature and increasing radiation as a result of evaporation processes, while the panel surface humidity shows a similar behavior as it decreases during periods of high radiation As a result of the surface temperature rising and then rising again in the evening with a decrease in radiation and an increase in atmospheric humidity, this behavior reflects the thermal and environmental interaction between solar radiation and humidity and their direct impact on the surface properties of solar panels.

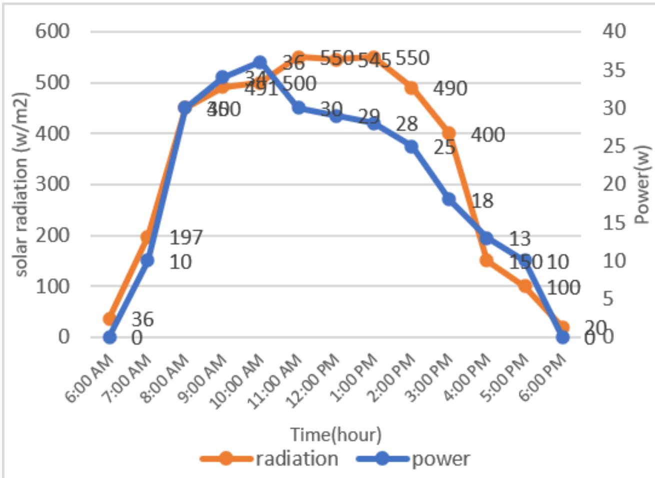

Figure 5. Time correlation between radiation intensity and output power

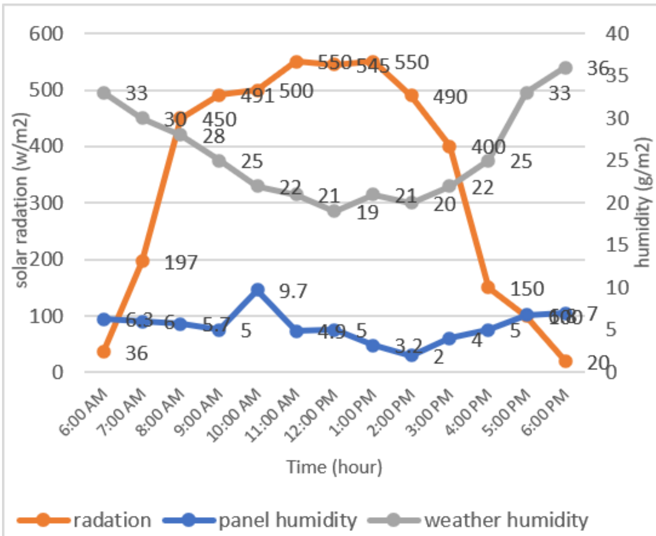

Figure 6. The daily relationship between solar radiation, solar panel humidity, and atmospheric humidity in terms of time

Calculations of solar radiation, solar panel temperature, and ambient temperature throughout the daytime hours are displayed in Figure 7. This data indicates solar radiation is available early in the morning, peaks at noon, and decreases gradually as we approach evening. When solar radiation strikes a solar panel, the panel's temperature is typically higher than the ambient air temperature. In fact, that increase can be significant. In contrast, the rise in ambient temperature is slower and smaller. From noon onwards, the panels cool down more quickly than the home air, either because of lower radiation intensity and/or greater heat loss from their outer surfaces. This shows how solar radiation affects panel temperature and illustrates the external weather conditions around this time of day that can skew that data.

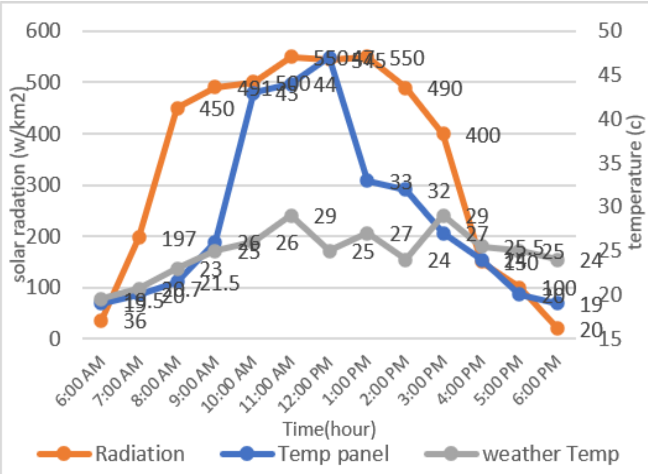

Figure 7. Daily change in solar radiation, solar panel temperature, and air temperature in terms of time

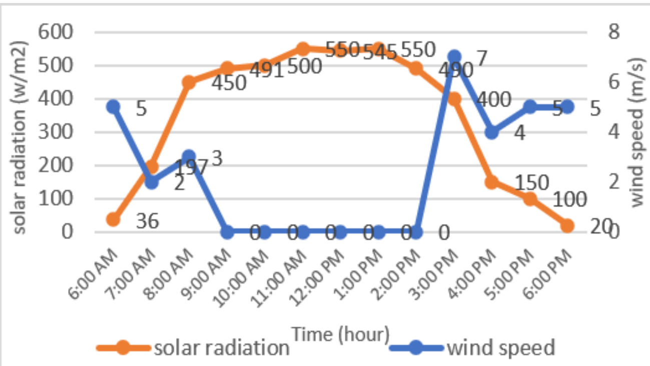

Figure 8. Daily change in wind speed and solar radiation

Figure 8 shows the daily variation of solar radiation and wind speed between 6:00 a.m. and 6:00 p.m. Solar radiation begins at approximately 36 W/m² around 6:00 a.m. and soon increases rapidly, reaching, on average, around 450 W/m² by 8:00 a.m., before gradually increasing to levels around solar noon, during the range of 11 a.m. to 1 p.m., with values from about 545 W/m² to 550 W/m². By now, radiation levels have been reduced further into the normal range, with a mean of about 150 W/m² at 4:00 p.m. and about 20 W/m² at around 6:00 p.m. That's where the sun takes its path through the sky. The wind speed, on the other hand, has a certain profile with a moderate 5 m/s speed at the origin (6:00 a.m.); it's gone down to 2–3 m/s almost every single time, again and again, at the same hour (7:00 and also 8:00 a.m.), and yes, it reaches its lowest (0 m/s) during time phases from continued up until the very recently mentioned time period (on the side of an exercise during one such era). That's after which there might as well have been some rise. But that means there is a certain quiet in the air when solar radiation is at its most intense. With a jump at 3:00 p.m., wind speeds rise to 7 m/s and settle down at 4–5 m/s by the end of the afternoon; heating and local convection explain the increase in wind speed around 3:00 p.m. It highlights the high temporal variability of solar radiation and wind speed, the intermittent nature of both aspects, and their corresponding effects on the performance of renewable energy systems over an average day.

Figure 9. Daily variation of photovoltaic (PV) output power (W) and output current (A) from 6:00 a.m. to 6:00 p.m.

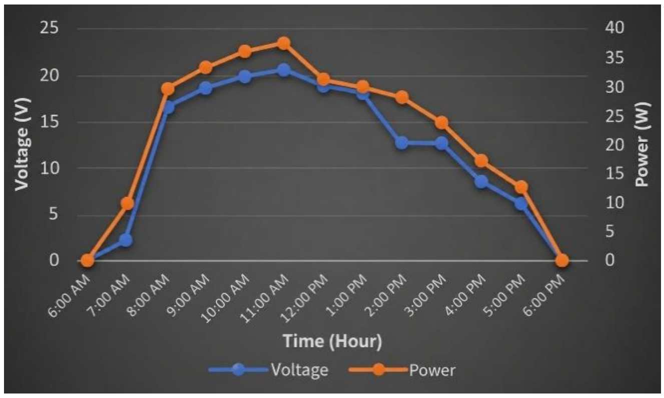

Figure 10. Daily variation of photovoltaic (PV) output voltage (V) and output power (W) from 6:00 a.m. to 6:00 p.m.

Figure 9 illustrates the daily behavior of both electrical power and output current based on experimental data, where values start near zero in the early morning hours and then rise significantly with increasing solar radiation intensity, reaching about 36 watts at 10 in the morning. In contrast, the current stabilizes at approximately 2.1 amperes. After that, the power and current gradually decrease throughout the afternoon and beyond as intensity, radiation, and plate temperature decrease. This behavior reflects the constant changes in the PV system's electrical operating conditions during daylight hours. illustrates in Figure 10 the daily behavior of the output voltage and electrical power as both parameters increase rapidly during the morning hours to reach peak values around 10:00 a.m. with the voltage approaching 20 V and the power around 22 W and then gradually decrease after midday as the voltage and power steadily decrease towards the afternoon and evening to reach nearly zero by 6:00 p.m., reflecting the direct dependence of the system outputs On the energy inputs available during the daily operating period.

As shown in Figure 9, the highest power output was achieved in the late morning. In contrast, the subsequent decrease in power and current indicates the combined effects of reduced solar radiation, high plate temperature, and gradual dust accumulation during the afternoon.

Figure 11 shows the daily change in the concentration of dust suspended in the air, dust deposition on the panels, and the capacity generated. Air dust concentrations begin at about 10 mg/m³ at 6:00 a.m., rise to an average of about 40 mg/m³ at 11:00 a.m., and then decrease significantly during the late afternoon. Airborne dust concentrations and dust concentrations on solar panels are shown daily, along with the predicted impact on power generation. Dust concentrations in the atmosphere begin at ~10 mg/m³ around 6:00 a.m., then increase to an average of ~40 mg/m³ at 11:00 a.m., and decrease significantly to ~2 mg/m³ by ~5:00 p.m. By comparison, deposition behavior on the panels is more predictable, peaking at ~34 mg/m² at 4:00 p.m., since the panels still accumulate dust and practically no removal occurs in the afternoon, compared with around 2 mg/m² in the morning. The power output, rising to 36 W at 10:00 a.m. (the a.m. start), has shown a steady trend as dust builds in the air and solar radiation increases. By the late afternoon, however, production gradually decreases towards approximately 3:00 p.m. and ~20 W, and the final output drops to almost 0 by the end of the day. Reduced transmission in direct sunlight is attributed to dust deposition on the PV panels reducing transmittance and the amount of solar radiation reaching the panels. Airborne dust particles will underperform panels sooner than settled dust because most of the dirt accumulates on panels in the afternoons. This highlights how often these require cleaning in order for the solar system to run at its maximum.

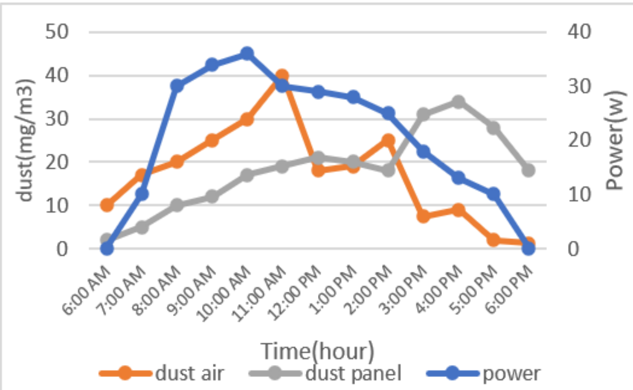

Figure 11. Daily variation of airborne dust concentration (mg/m³), panel dust deposition (mg/m²), and generated power (W) from 6:00 a.m. to 6:00 p.m.

According to measured data, dust accumulation on the plate surface increased from about 2 mg/m² in the morning to about 34 mg/m² in the late afternoon, accompanied by a significant decrease in production capacity. These results suggest that the cleaning process should be performed when dust accumulation reaches 30 mg/m². From the collected data, considering the recorded conditions, this equals about one cleaning cycle per 1–2 days during dusty periods. In addition to periodic cleaning, dust mitigation measures are preventive measures such as anti-soiling coatings, self-cleaning hydrophobic surfaces, and increased angles on panel inclination to limit dust adhesion. Such technologies also aid in diminishing optical losses and the volume of maintenance work per day, particularly in dry environmental conditions.

The main observation in Figure 11 is that during dust deposition on the panel surface, the amount of generated power diminishes as the dust deposit rises and is in fact very close to the maximum measured value. This means that they should wash or use Anti-Soiling Mitigation Techniques if dust accumulates and/or is needed; this is an acceptable operational aspect. Furthermore, the findings also show that PV performance is influenced by the combined effect of environmental stressors as opposed to each factor alone. High plate temperature leads to low effectiveness as a means of electric conversion, and dust accumulation decreases the optical transmittance. When the two are present simultaneously, the power loss increases. The measured power was reduced from about 36 W to approximately 13 W as dust deposition reached its maximum measurement value of approximately 34 mg/m² due to the combined effects of dust accumulation, heat stress, and suppressed solar radiation emitted during the afternoon. The simultaneous presence of relatively high humidity and dust during the early hours of the morning may enhance particle adhesion to the panel surface, reducing light penetration, increasing monitoring and cleaning work on the panels for dust-infested climates.

A simplified mathematical model may be constructed that explains the quantitative relationships between output power and these primary environmental factors with respect to solar radiation intensity, panel surface temperature, and dust buildup. This relationship can be deduced in a simpler version in Eq. (1), which contains positive radiation-related cross-line energy entering the system, whilst negative effects are introduced into the system, such as high temperature, which leads to low electrical efficiency, and increased dust accumulation, which leads to a decrease in optical permeability. According to this model, the capacity generated does not come from any single component but from the intricate interdependences between ecosystem components that regulate the functioning of the system in the environment [21, 22].

$$P = k \cdot G \cdot (1 - \beta(T_{\mathrm{p}} - Tref)) \cdot (1 - \gamma D) \quad (1)$$

3.2 Forecast data with realistic data results

Figure 12 shows a rigorous evaluation of the credibility of meteorological data, real vs. expected values for humidity and wind speed throughout the day. The actual humidity curve illustrates s a concave behavior that starts with high values in the morning at 33 g/m^2 and then gradually descends to reach its lowest levels at noon, recording about 18 g/m^2 as a result of rising temperatures and evaporation of suspended humidity before rising again to reach 36 g/m^2 in the evening. The predictive data for humidity simulate the same directional path, but with lower values, reflecting a fixed margin of error in the estimate. As for wind speed, the real data revealed a period of stagnation and complete stillness during which the speed disappeared to reach zero in the period extending from nine in the morning until two in the afternoon, which the predictive data failed to detect, as the speed during that period was estimated at an average of 3–5 m/s.

Figure 13 reveals that the imported atmospheric data matches the actual reality of radiation and temperature; as you can tell in this figure, the solar radiation values differ fundamentally: the predictive model used (in yellow) overestimated its output, peaking at about 660 W/m² around 12 o'clock in the afternoon, whereas the actual results (in orange) show that the actual irradiance was below 550 W/m². This difference could be due to local environmental conditions—such as dust or passing clouds—that didn't enter the forecasts. For the temperature data, relative convergence is observed along the general path. However, actual readings fluctuate, dipping slightly from 2:00 p.m. to 24 °C, while the prediction curve displays more moderate and stable values.

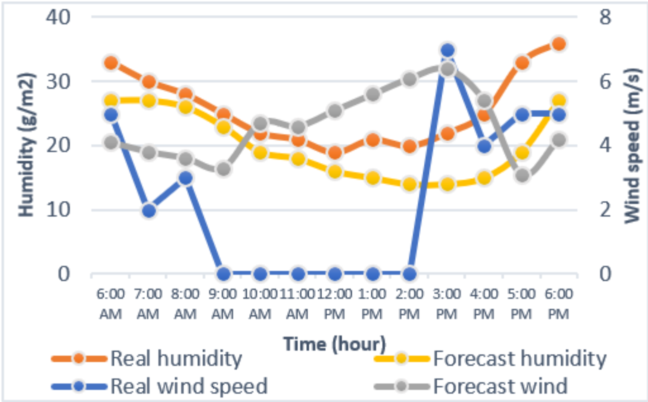

Figure 12. Daily comparison between measured and expected values of humidity and wind speed in terms of time

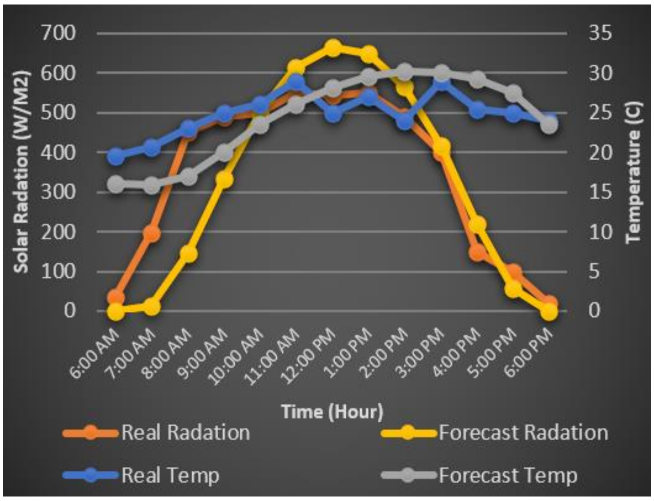

Figure 13. Analysis of the standard gap between realistic and predictive data for solar radiation rates and temperatures

The higher-than-real estimate of projected solar radiation values is mainly due to subtle local climatic factors that are not fully represented in large-scale atmospheric models. These factors include dust concentration, temporary shading, Atmospheric Aerosols, and site-specific environmental conditions.

The accuracy of predictions can be improved in the future by integrating local sensor measurements into the prediction process and applying machine learning-based correction models trained on historical measurements and past predictions.

Integrating forecast data with real-time measurements enhances PV performance monitoring by enabling direct comparison between forecasted and actual operating conditions. This approach enables the identification of local environmental impacts, such as dust accumulation and microclimate changes, that large-scale forecast models cannot fully represent, thereby contributing to more efficient and accurate performance assessment and maintenance planning. The discrepancy between the forecast and measured data indicates a systematic overstatement by the forecast model, particularly in solar radiation. In this study, the Root Mean Square Error (RMSE) was about 85 W/m². In comparison, the Mean Absolute Error (MAE) was about 72 W/m², which confirms that the model was unable to represent local operating conditions fully. The main sources of this bias may include local dust, Atmospheric Aerosols, temporary shading, wind stagnation near the Earth's surface, and microclimatic influences surrounding the test site. Therefore, forecasting models for PV applications in dry areas should be improved by incorporating high-spatial-resolution weather data, local dust measurements, and real-time feedback from local sensors. Future models could also rely on machine learning-based correction algorithms trained using measured and forecast data to reduce forecast bias and improve the reliability of results.

3.3 Optical monitoring and digital processing system

Table 2 illustrates the analytical outputs of a direct optical monitoring system, in which an installed electronic camera scans the solar panel's surface and processes images algorithmically to determine dust accumulation rates and any optical distortions that may impede optical absorption. The embedded data illustrates the system's response to different test scenarios, with the first image recording the highest observed distortion rate. This is due to a deliberate sensitivity test in which white pieces were placed on the plate surface to verify detection accuracy. The table also highlights a special case in which strong reflections of sunlight appear on the surface of the painting, as the camera deals with it and reads it as a distortion ratio, which explains the mechanism of the system's work in classifying any change in the optical homogeneity of the surface, whether physical, such as dust and foreign objects, or optical, such as sharp reflections.

The optical monitoring system adds another method for consumers to monitor the health of their panels. Unlike ordinary electrical measurements, its features allow anyone to monitor the panels' surfaces at all times. By implementing image processing features, it's much easier to notice things like dust, foreign objects, or strong reflections — things that electrical checks might ignore. This helps users find faults early and plan maintenance, since they can actually see the panel's condition. In large PV setups, the system also has high ease of use. This is a low-cost option for real-time monitoring and predictive maintenance – especially in dusty areas where surface dirt may seriously hinder performance or the efficiency of equipment.

3.4 Statistical analysis paragraph

The statistical assessment was utilized to determine the correlation between the environmental variables and the electrical performance of the PV system. Pearson's correlation coefficient was employed to measure the strength of the relationship between solar radiation, panel temperature, dust accumulation, and production capacity. Such a tendency is supported by the output data; for the two variables, production and solar intensity, the correlation is significantly similar ($r = 0.91$), which means that the production of power is mainly from solar input. In contrast, high panel temperature was only moderately negatively related to the system's production capacity (−0.6336), confirming that high temperatures reduce system yield even when there is considerable radiation. Dust deposition on the surfaces of the panels also negatively correlated with production capacity, demonstrating that deposition of dust is not only detrimental to the transmittance of light but also impacts productivity at various points of the day — notably in the afternoon, when dust accumulation is most inevitable. Wind speed had a weak positive correlation with production capacity (~0.32), suggesting that surface cooling from wind slightly improved performance but also measured performance. Errors (the difference between observed and predicted) were used to measure prediction accuracy. The intercept values for solar radiation were 85 W/m² with RMSE, with an MAE of about 72 W/m² indicating that the predictive data could be overestimated. The differences have been attributed to more local environmental conditions (dust, microclimates) that general predictive models do not consider. Generally speaking, these evaluations support the observation of solar radiation as the major force of energy generation while temperature and dust build-up are its principal challenges. All of these were significant points indicating that the performance in desert conditions was only sustained by good thermoregulation and frequent cleaning of the surface.

This dataset was chosen as the most representative observation day, since it demonstrated maximum completeness and encapsulated most of the response behaviour of the PV system to environmental changes across multiple measurement days. The findings indicated that the PV unit's power output was dependent on solar energy. Meanwhile, panel temperatures above around 40 °C displayed a significant reduction in power output even with ample solar irradiance. Likewise, as dust accumulation on the panel surfaces increased, energy generation decreased, especially when deposition was near the greatest readings during that observation time. Temperature control and minimizing dust collection were mentioned as crucial parameters to achieve the best performance of PV systems in these scenarios. Future work could be performed using large, multi-day datasets, as well as developing predictive models using Regression and machine learning models to pinpoint reliable operational limits and scenarios that have improved cooling with less dust settling on solar panels.

Table 2. Analytical data for digital camera outputs

Date	Name	Image	Result
29/11/2025	15-42-25	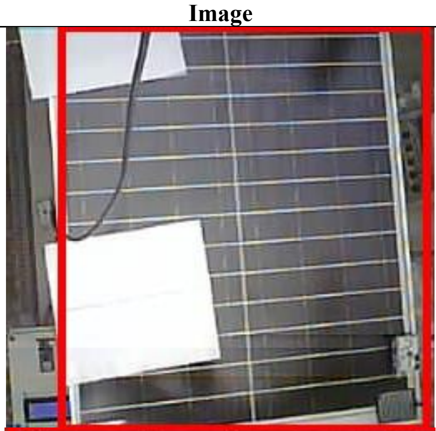	0.6198
29/11/2025	15-49-19		0.4946
13/11/2025	12-34-47		0.2531

14/11/2025	09-11-36		0.5911
15/11/2025	14-10-30		0.4521

3.5 Summary

Field data and comparisons with previously published data indicate that environmental conditions, namely temperature, solar irradiance, and humidity, are the primary bottlenecks for high-efficiency Monocrystalline PV systems. These factors interact in several key ways that are clearly evident in both empirical (observed) and predictive (modeled or estimated) data. The data illustrates that the increase in the temperature of the panel, despite its coincidence with the increase in radiation intensity, leads to a decrease in the produced power as a result of the negative thermal effect on the electrical efficiency, which explains why the power reaches its maximum values in the late morning period before it starts By decreasing despite the continued rise in radiation, the results also illustrates that the accumulation of dust on the surface of the plate represents one of the most influential factors in the daily term, as it leads to a reduction in optical transmittance and thus a significant reduction in productivity, especially in the afternoon hours, when accumulation is at its highest levels, while wind speed contributed Limitedly to improving performance by enhancing surface cooling, while the effect of humidity was linked to a change in the optical properties of the surface as a result of the formation of Moisture layers affect radiation absorption. In contrast, when comparing measured data with forecast data, a significant gap was identified in the representation of radiation intensity and wind behavior, indicating that local features, including dust and microclimatology, are not captured in higher-resolution models. This underscored the need to use real measurements to ensure fair performance metrics. The system was operated, and data were collected for several days in November to build a database. It represents the change in operating conditions. Still, the day presented in the analysis was chosen because it represents the most obvious case in terms of recording the highest values of solar radiation, which allows highlighting the physical effects of environmental factors more accurately and enhances the reliability of interpreting the system behavior under relatively extreme loading conditions, which provides a deeper understanding of the relationship between climate variables and electrical performance and contributes to supporting operation and maintenance decisions in hot and dry environments.

Compared to currently available real-time PV monitoring systems, the proposed system provides broader diagnostic capabilities by integrating electrical, environmental, dust-related, optical, and predictive data into a single platform. The use of predictive data also enhances the effectiveness of practical monitoring by providing a reference for expected performance. At the same time, real-time measurements reveal actual deviations resulting from local operating conditions. Therefore, the system supports a more accurate assessment of PV system performance and helps make maintenance decisions more efficiently and reliably.

Thus, although this research is carried out in Baghdad, such findings are of relevance to other arid and semi-arid areas that are also subjected to the same environmental stresses such as high temperatures, intense solar radiation, frequent dust storms, and low rainfall. These conditions are widespread in many countries of the Middle East and North Africa, including Saudi Arabia, the United Arab Emirates, and other desert areas, where PV systems undergo similar operational issues. But Baghdad suffers from frequent dust storms and large suspended particle concentrations in the air, and local urban environmental impacts, which can influence the degree of operational performance losses. Hence, the recommended monitoring method can be applied to areas that have similar climates. Nevertheless, the quantitative results should be interpreted in the context of local environmental conditions at each site. From a performance perspective, it’s concluded that regular cleaning of the panel is necessary in dusty conditions because it should help to prevent a performance loss as a result of dust on the surface. By monitoring panel temperatures, periodic monitoring of panel temperature provides time-scale observations that indicate extreme thermal impacts on the system, reducing electrical efficiency. As a result, PV system operators in hot, dry climates should keep preventative maintenance strategies that are related to periodic cleaning, constant environmental monitoring, and suitable panel installation to promote natural cooling and decrease dust build-up. These measures may promote system dependability and stable power production in challenging environmental scenarios.

3.6 Limitation

When interpreting the results, the study encompasses several determinants. On the one hand, while the sensors were installed and operated on the ground, the measurement uncertainties could originate from the calibration process on the sensors, direct environmental contact, as well as the harsh climatic conditions of Baghdad, namely high temperature and dust. Secondly, the detailed analysis shown in this study was based on data collected in the month of November, and the selected observation day is the most complete and representative dataset among multiple observation days. Accordingly, it is possible that the reported results do not reflect seasonal variations in ambient (weather-related) conditions or PV system operation. Future work should extend the monitoring period into additional chapters and longer-term datasets, allowing a more exhaustive validation of the proposed monitoring and forecasting framework and determination of its overall performance under different operating and environmental situations.

4. CONCLUSION

The results indicate that the performance of PV systems is greatly affected by environmental factors, especially temperature and dust accumulation, as high temperature reduces electrical efficiency despite the availability of high solar radiation, while dust represents the factor that most affects daily performance as a result of its direct effect on reducing optical transmittance and reducing the production capacity. It was also shown that wind speed contributes to improved performance to a limited extent by enhancing cooling, while it affects surface moisture properties, thereby reducing light absorption. This difference was substantial between the actual and predictive values. This motivates the need to evaluate hardware performance using real measurements. It is based on Arduino and ESP32 controllers, which provide high-efficiency real-time monitoring and analysis. This system is a beneficial tool for optimizing operational and maintenance strategies and improving the performance of solar energy systems placed in hot, arid regions.

ACKNOWLEDGMENT

The researchers express their sincere appreciation and gratitude to the Department of Electromechanical Engineering at the University of Technology, Iraq, for the scientific cooperation and technical support provided, which played an important role in completing this study and ensuring it was carried out as required.

REFERENCES

[1] Hassan, S., Jadallah, A., Bilal, G. (2023). Design and implementation of a smart greenhouse automated and conditioned by solar power system. Engineering and Technology Journal, 41(1): 37-44. https://doi.org/10.30684/etj.2021.131279.1024

[2] Bilal, G.A., Jadallah, A.A., Abdulmajeed, O.M., Arıcı, M. (2025). Fluid flow characteristics estimation of a new integrated bifluid/airbased photovoltaic thermal system utilizing a hybrid optimization method. International Journal of Thermofluids, 25: 101034. https://doi.org/10.1016/j.ijft.2024.101034

[3] Mahdi, B.S., Abdul Hassan, A.K. (2015). Hybrid techniques for proposed intelligent digital image watermarking. Engineering and Technology Journal, 33(4): 702-713. https://www.uotechnology.edu.iq/tec_magaz/2015/volum332015/No.04.B.2015/Text(13).pdf.

[4] Ismaeel, A.A., Wahhab, H.A.A., Naji, Z.H. (2021). Performance evaluation of updraft air tower power plant integrated with double skin solar air heater. Evergreen, 8(2): 296-303. https://doi.org/10.5109/4480706

[5] Hassan, S.H., Bilal, G.A., Ismaeel, A.A. (2026). Methodological design and performance simulation of a 25 MW grid-connected solar PV plant using PVsyst. Engineering and Technology Journal, 44(2): 23-39. https://doi.org/10.30684/2412-0758.1016

[6] Hadi, H.A., Kassem, A., Amoud, H., Nadweh, S., Ghazaly, N.M. (2024). Using grey wolf optimization algorithm and whale optimization algorithm for optimal sizing of grid-connected bifacial PV systems. Journal of Robotics and Control (JRC), 5(3): 733-745. https://doi.org/10.18196/jrc.v5i3.21777

[7] Hussain, A., Batra, A., Pachauri, R. (2017). An experimental study on effect of dust on power loss in solar photovoltaic module. Renewables: Wind, Water, and Solar, 4: 9. https://doi.org/10.1186/s40807-017-0043-y

[8] Hashim, B.M., Sultan, M.A., Al Maliki, A., Al-Ansari, N. (2020). Estimation of greenhouse gases emitted from energy industry (oil refining and electricity generation) in Iraq using IPCC methodology. Atmosphere, 11(6): 662. https://doi.org/10.3390/atmos11060662

[9] Bamisile, O., Acen, C., Cai, D.S., Huang, Q., Staffell, I. (2025). The environmental factors affecting solar photovoltaic output. Renewable and Sustainable Energy Reviews, 208: 115073. https://doi.org/10.1016/j.rser.2024.115073

[10] Chala, G.T., Sulaiman, S.A., Al Alshaikh, S.M. (2024). Effects of climatic conditions of Al Seeb in Oman on the performance of solar photovoltaic panels. Heliyon, 10(10): e30944. https://doi.org/10.1016/j.heliyon.2024.e30944

[11] Hashim, S.M., Hassan, R.I. (2022). Impact of high temperature on PV productivity in hot desert climates. Green Technology, Resilience, and Sustainability, 2: 9. https://doi.org/10.1007/s44173-022-00009-9

[12] Jaffar, M.F., Ahmed, A.Q., Mohammad, A.T., Al-Shohani, W.A.M. (2022). Performance evaluation of the

polycrystalline photovoltaic module under Iraqi harsh weather conditions. International Journal of Advanced Technology and Engineering Exploration, 9(88): 257-269. https://doi.org/10.19101/IJATEE.2021.875255
[13] Fernandez, A.A., Rakhmatsyah, A., Wardana, A.A. (2020). Monitoring floating solar tracker based on axis coordinates using LoRa network. International Journal of Renewable Energy Development, 9(2): 141-149. https://doi.org/10.14710/ijred.9.2.141-149
[14] Chen, J.X., Pan, G.B., Ouyang, J., Ma, J., Fu, L., Zhang, L.B. (2020). Study on impacts of dust accumulation and rainfall on PV power reduction in East China. Energy, 194: 116915. https://doi.org/10.1016/j.energy.2020.116915
[15] Chanchangi, Y.N., Ghosh, A., Sundaram, S., Mallick, T.K. (2020). Dust and PV performance in Nigeria: A review. Renewable and Sustainable Energy Reviews, 121: 109704. https://doi.org/10.1016/j.rser.2020.109704
[16] Coskun, C., Toygar, U., Sarpdag, O., Oktay, Z. (2017). Sensitivity analysis of implicit correlations for photovoltaic module temperature: A review. Journal of Cleaner Production, 164: 1474-1485. https://doi.org/10.1016/j.jclepro.2017.07.080
[17] Abiola-Ogedengbe, A., Hangan, H., Siddiqui, K. (2015). Experimental investigation of wind effects on a standalone photovoltaic (PV) module. Renewable Energy, 78: 657-665. https://doi.org/10.1016/j.renene.2015.01.037
[18] Mahmood, A.L., Shakir, A.M., Numan, B.A. (2020). Design and performance analysis of stand-alone PV system at Al-Nahrain University, Baghdad, Iraq. International Journal of Power Electronics and Drive Systems, 11(2): 921-930. https://doi.org/10.11591/ijpeds.v11.i2.pp921-930
[19] Bahadori, A., Nwaoha, C. (2013). A review on solar energy utilisation in Australia. Renewable and Sustainable Energy Reviews, 18: 1-5. https://doi.org/10.1016/j.rser.2012.10.003
[20] Jaffar, H.A., Ismaeel, A.A., Shuraiji, A.L. (2025). Optimizing and developing a new model for SVE through simulation and experimentation to improve PV. Renewable Energy, 247: 123010. https://doi.org/10.1016/j.renene.2025.123010
[21] Rout, K.C., Kulkarni, P. (2020). Design and performance evaluation of proposed 2 kW solar PV rooftop on-grid system in Odisha using PVsyst. In 2020 IEEE International Students' Conference on Electrical, Electronics and Computer Science (SCEECS), Bhopal, India, pp. 1-6. https://doi.org/10.1109/SCEECS48394.2020.124
[22] Ndiaye, E.H.M., Ndiaye, A., Faye, M., Gueye, D., Ba, A., Traore, M. (2025). Analysis of the impact of irradiance and temperature on photovoltaic production: A statistical and machine learning approach. MethodsX, 15: 103716. https://doi.org/10.1016/j.mex.2025.103716

NOMENCLATURE

P	Output electrical power, W
G	Solar irradiance, W/m²
Tp	Panel surface temperature, °C
Tref	Reference temperature, °C
D	Dust accumulation on panel surface, mg/m²
k	Proportional constant
β	Temperature coefficient, 1/°C
γ	Dust loss coefficient
Voc	Open circuit voltage, V
Isc	Short circuit current, A
Vmpp	Voltage at maximum power point, V
Impp	Current at maximum power point, A
η	Efficiency of PV module, %
GET	Hypertext Transfer Protocol (HTTP) GET Request
JSON	JavaScript Object Notation
UART	Universal Asynchronous Receiver/Transmitter
LCD	Liquid Crystal Display
CSV	Comma-Separated Values
SD	Secure Digital